

# High-Entropy Metallic Glasses

W.H. WANG<sup>1,2</sup>

1.—Institute of Physics, Chinese Academy of Sciences, Beijing 100190, People's Republic of China.  
2.—e-mail: whw@iphy.ac.cn

The high-entropy alloys are defined as solid-solution alloys containing five or more than five principal elements in equal or near-equal atomic percent. The concept of high mixing entropy introduces a new way for developing advanced metallic materials with unique physical and mechanical properties that cannot be achieved by the conventional microalloying approach based on only a single base element. The metallic glass (MG) is the metallic alloy rapidly quenched from the liquid state, and at room temperature it still shows an amorphous liquid-like structure. Bulk MGs represent a particular class of amorphous alloys usually with three or more than three components but based on a single principal element such as Zr, Cu, Ce, and Fe. These materials are very attractive for applications because of their excellent mechanical properties such as ultrahigh (near theoretical) strength, wear resistance, and hardness, and physical properties such as soft magnetic properties. In this article, we review the formation and properties of a series of high-mixing-entropy bulk MGs based on multiple major elements. It is found that the strategy and route for development of the high-entropy alloys can be applied to the development of the MGs with excellent glass-forming ability. The high-mixing-entropy bulk MGs are then loosely defined as metallic glassy alloys containing five or more than five elements in equal or near-equal atomic percent, which have relatively high mixing entropy compared with the conventional MGs based on a single principal element. The formation mechanism, especially the role of the mixing entropy in the formation of the high-entropy MGs, is discussed. The unique physical, mechanical, chemical, and biomedical properties of the high-entropy MGs in comparison with the conventional metallic alloys are introduced. We show that the high-mixing-entropy MGs, along the formation idea and strategy of the high-entropy alloys and based on multiple major elements, might provide a novel approach in search for new MG-forming systems with significances in scientific studies and potential applications.

## INTRODUCTION

Since the discovery of the glassy AuSi alloys in 1960s,<sup>1</sup> intensive efforts had been made in the development of metallic glasses (MGs) because of their excellent properties such as high strength near the theoretical prediction, high hardness, large elastic strain, high corrosion and wear resistances, and unique physical properties (such as excellent soft magnetic properties) compared with their crystalline counterparts.<sup>2–6</sup> In the early stage, the exploration of the MG systems was based on the techniques of the rapid metallic melt quenching,

which can kinetically bypass the process of nucleation and growth of crystalline phases in some alloy melts and yield a configuration frozen liquid of MG. The extensively developed and elaborated rapid quenching techniques for chilling metallic liquids at very high rates of  $10^5$ – $10^6$  K/s have produced a wide variety of MG systems. However, the technique associated with such ultrahigh cooling rates has restricted the MG production to the forms of ribbons, wire, or droplets with microscale cross section.<sup>2–6</sup>

Through careful composition design, MGs with much larger three-dimensional size and exceptional

high glass-forming ability (GFA)<sup>7–10</sup> were developed in the 1990s with a relatively low critical cooling rate of 1–100 K/s. Inoue<sup>8</sup> found that the alloys of the families La-Al-TM (TM represents a transition metal), Mg-TM-RE (RE represents a rare-earth metal), and Zr-Al-TM could be cast (e.g., simple water quenching or conventional copper mold cast) to form cylinders and plates a few millimeters in cross section. Later, it was found that much better GFA could be obtained in some alloy systems with more than three components [e.g.,  $Zr_{65}Al_{7.5}Ni_{10}Cu_{17.5}$  (Ref. 8) and  $(Cu_{50}Zr_{50})_{92}Al_7Gd_1$  (Ref. 11)]. With the addition of beryllium with small atomic size, a  $Zr_{41}Ti_{14}Cu_{12.5}Ni_{10}Be_{22.5}$  alloy with the anomalously easy GFA was developed.<sup>7</sup> One can see that the key for the success is just the compositional complexity.<sup>12</sup> However, the advance for MG field is great, and a lot of multicomponent bulk MGs such as Fe-, Mg-, Zr-, Ti-, Cu-, Fe-, Ta-, Zn-, Ca-, Sr-, Sc-, and rare-earth-based alloys have been successfully fabricated since then.<sup>10–30</sup> A so-called “confusion principal”<sup>12</sup> has been proposed and seems to have been widely accepted for the search of MGs with good GFA because a mixture of elements with various atomic radii could lead to dense packing in the melt state, and the resulting stability favors the glass formation against crystallization.<sup>7,8,12</sup> It is also found that other factors including the numbers and atomic size of the constituent elements as well as the mixing enthalpy between the main elements also play important roles for the MG formation.<sup>3</sup>

It is emphasized that the main design strategy of these multi-component bulk MGs is based on a single element such as Zr, Mg, Cu, and Fe. Generally, the way for developing bulk MGs is to select one element as a base component and some other elements to match the base element for obtaining a good GFA,<sup>3,7,8,10</sup> and this limits the development of more MG systems. To break through the traditional strategy of alloy design, some bulk MGs based on multiple major elements such as  $Zr_{50}Cu_{50}$ -based or LaCe-based bulk MGs and  $(Ti_{33}Zr_{33}Hf_{33})_{40}(Ni_{50}Cu_{50})_{50}Al_{10}$  in ribbon form by melt spinning were developed, and these MGs are alloys with a combination of more than two major elements.<sup>11,15,17,18,31–33</sup>

Recently, a new type of advanced solid-solution metallic alloys, defined as high-entropy alloys by Yeh et al.<sup>34</sup> and named by Cantor et al.<sup>35</sup> as multicomponent alloys, that contain five or more than five principal elements in equal or near-equal atomic percent have attracted increasing attentions because of their unique compositions, microstructures, and adjustable properties.<sup>36–40</sup> These crystalline multicomponent equimolar alloys (the atomic fraction of each component is greater than 5 at.%) are normally located at the center of a multicomponent phase diagram, and their configuration entropy of mixing reaches its maximum for a solution phase.<sup>36</sup> In the metallurgy field, a conventional alloy development strategy, which had been

used for a thousand years, has led to an enormous amount of knowledge about alloys based on one or two components, but there is little knowledge about alloys containing several main components in near-equal proportions. The concept and the strategy of high-entropy provide a new route or idea for developing new alloys with unique physical and mechanical properties, and these new alloys have great potential to be used as high-temperature materials, coating materials requiring high hardness and high wear resistance, and corrosion-resistant materials with high strength.<sup>36–40</sup> Intensive work has been done recently on the fundamental understanding of high-entropy alloy formation.<sup>36–43</sup>

One can see that the two types of metallic materials of bulk MGs and the crystalline high-entropy alloys have a common characteristic of complexity: More elements involved in an alloy could induce unique features, which is to play on the “more is different” theme.<sup>44</sup> However, high-entropy alloys and bulk MGs have been independently studied. They exhibit considerably different characteristics in their alloy systems, compositions, atomic structure, processing, and even features and properties. The intriguing question is why has there been so few attempts to exploit the concept and the strategy of high-entropy in MGs field. One answer seems to be that the scientists in MGs community are reluctant to deal with the complicated alloys: The more elements, the more difficult the analysis of the relaxation, structure, relation between structure and properties, and thermodynamics and kinetics of the glassy alloys formation. Another answer could be that the scientists in MG community have long been believed that the properties of the alloys are determined by the principal element, and thus, the solute elements are added to enhance the properties of the solvent element.

Recently, the experimental results demonstrate that the concept and the strategy of the high entropy, when applied with care, works effectively in the development of novel MGs with excellent GFA and unique features and properties.<sup>45–51</sup> This might make people come to recognize the role of complexity in glassy alloys formation. Another intriguing question is why do solid solutions or the glassy phases form in multicomponent alloys with high mixing entropies? The scientific scheme capable of predicting the formation of solid solutions with stable and crystalline structure or the MG with metastable and disordered structure is of both scientific and technical significance. It is anticipated that the application of the high-entropy idea in MG field could also have implications for the scientific understanding toward the formation mechanism of the high-entropy alloys, which lags much behind the technical exploration to them.<sup>36</sup> In the multicomponent MG-forming alloy systems, the formation mechanism and criterion for the glassy phase and not the more thermodynamically stable intermetallic compounds have been intensively studied.<sup>2–4</sup>

However, the questions why the metastable MGs or the solid-solution phases and not the stable inter-metallic compounds form in these highly concentrated multicomponent alloys is still unclear.

In this article, we attempt to loosely define the high mixing entropy bulk MGs and summarize the formation and properties of the so far available high-entropy bulk MGs based on multiple major elements. It is demonstrated that the strategy and route for development of the high-entropy alloys can be used to develop a series of MGs with excellent GFA and unique properties. The formation mechanism, especially the role of the mixing entropy in the glass formation of the high-entropy MGs, is discussed. The unique physical, mechanical, chemical, and biomedical properties of the high-entropy MGs in comparison with conventional metallic alloys are introduced. We show that the high-mixing-entropy MGs, along the formation idea and strategy of the high-entropy alloys and based on multiple major elements, might provide a novel and effective approach for the design and search of new MG-forming alloy systems with significances in scientific studies and potential applications.

## FORMATION AND FORMATION CRITERIA

### The Formation of the High Mixing Entropy MGs

Along the idea of multi-component and equimolar of the formation of high-entropy alloys, a series of high-mixing-entropy bulk MGs have been successfully produced.<sup>45–51</sup> The available typical high-mixing-entropy MGs systems are listed in Table I.

The systems involved in the transition metals such as Zr, Sr, Ca, Ti, and Cu, metalloids such as B and Si, and rare-earth metals such as Er, Yb, Tb, and Dy, as well as Al and Mg. All of them are conventional bulk MG-forming components. However, one can see that their critical sizes or GFA are quite different even though these alloys have similar mixing entropy, which indicates the GFA of an alloy is not solely determined by the mixing entropy. The high mixing entropy is neither a sufficient condition

nor a necessary condition for the formation of the bulk MGs because the high mixing entropy does not always lead to the formation of the fully glassy phase. The high-entropy effect is mainly related to the well-known confusion principle for the glass formation.

From Table I, we know that the known high-entropy MG systems can be produced by almost all available MG-forming methods including copper mold cast, melt spinning, mechanical alloying, fluxed water quenching, and so on. As an example, we show the preparation procedure of the high-entropy  $\text{Sr}_{20}\text{Ca}_{20}\text{Yb}_{20}\text{Mg}_{20}\text{Zn}_{20}$  bulk MGs. The Sr (99.0%), Ca (99.0%), Zn (99.9%), Mg (99.9%), and Yb (99.0%) elements were selected. By melting mixtures of these elements using induction-melting method in a quartz tube under vacuum (better than  $3.0 \times 10^{-3}$  Pa) and subsequently casting into copper mold, the fully glassy alloy in cylindrical shape (50 mm in length) or in plate form with shiny metallic surfaces were obtained.<sup>46</sup> The structures of the as-cast alloys were examined by x-ray diffraction and a Mettler-Toledo differential scanning calorimeter DSC822e (Mettler-Toledo LLC, Columbus, OH) with a heating rate of 10 K/min under a continuous argon flow. The glass transition temperatures ( $T_g$ ), onset temperatures of the crystallization event ( $T_x$ ), and liquidus temperature  $T_l$  were determined from the thermal analysis traces. Figure 1 shows the XRD patterns of as-cast  $\text{Sr}_{20}\text{Ca}_{20}\text{Yb}_{20}\text{Mg}_{20}\text{Zn}_{20}$ ,  $\text{Sr}_{20}\text{Ca}_{20}\text{Yb}_{20}(\text{Li}_{0.55}\text{Mg}_{0.45})_{20}\text{Zn}_{20}$ , and  $\text{Sr}_{20}\text{Ca}_{20}\text{Yb}_{20}\text{Mg}_{20}\text{Zn}_{10}\text{Cu}_{10}$  alloys. For the alloys in plate form with the dimensions of  $2 \times 5 \text{ mm}^2$ , the typical halo patterns for the amorphous phase were obtained and no diffraction peaks could be resolved within the resolution limit of the XRD. The fully glassy  $\text{Sr}_{20}\text{Ca}_{20}\text{Yb}_{20}\text{Mg}_{20}\text{Zn}_{10}\text{Cu}_{10}$  alloy in the rod with a diameter up to 5 mm could be obtained by the copper mold cast.

Figure 2 shows the DSC curves of as-cast high-entropy  $\text{Sr}_{20}\text{Ca}_{20}\text{Yb}_{20}(\text{Li}_{0.55}\text{Mg}_{0.45})_{20}\text{Zn}_{20}$ ,  $\text{Sr}_{20}\text{Ca}_{20}\text{Yb}_{20}\text{Mg}_{20}\text{Zn}_{10}\text{Cu}_{10}$ , and  $\text{Sr}_{20}\text{Ca}_{20}\text{Yb}_{20}\text{Mg}_{20}\text{Zn}_{20}$  MGs. Each DSC curve exhibits an apparent endothermic event associate with glass transition and a

**Table I. The Typical high-entropy bulk MG systems**

System	Critical size (mm)	Method	Year	Reference
$\text{Zn}_{20}\text{Ca}_{20}\text{Sr}_{20}\text{Yb}_{20}(\text{Li}_{0.55}\text{Mg}_{0.45})_{20}$	> 3	Copper mold casting	2011	45
$\text{Sr}_{20}\text{Ca}_{20}\text{Yb}_{20}\text{Mg}_{20}\text{Zn}_{20}$	4	Copper mold casting	2011	46
$\text{Sr}_{20}\text{Ca}_{20}\text{Yb}_{20}\text{Mg}_{20}\text{Zn}_{10}\text{Cu}_{10}$	5	Copper mold casting	2011	46
$\text{Er}_{20}\text{Tb}_{20}\text{Dy}_{20}\text{Ni}_{20}\text{Al}_{20}$	2	Copper mold casting	2011	46
$\text{Pd}_{20}\text{Pt}_{20}\text{Cu}_{20}\text{Ni}_{20}\text{P}_{20}$	10	fluxed water quenching	2011	48
$\text{Ti}_{20}\text{Zr}_{20}\text{Cu}_{20}\text{Ni}_{20}\text{Be}_{20}$	3	Copper mold casting	2013	50
$\text{Fe}_{20}\text{Si}_{20}\text{B}_{20}\text{Al}_{20}\text{Ni}_{20}$	Powders	Ball milling	2013	49
$\text{Fe}_{20}\text{Si}_{20}\text{B}_{20}\text{Al}_{20}\text{Nb}_{20}$	Powders	Ball milling	2013	49
$\text{AlCoCrFeNiZr}_{0.6}$	Ribbon	Melt spinning	2014	51
$\text{CoCrCuFeNiZr}_{0.6}$	Ribbon	Melt spinning	2014	51
$\text{Ti}_{20}\text{Zr}_{20}\text{Hf}_{20}\text{Cu}_{20}\text{Ni}_{20}$	1.5	Copper mold casting	2002	52

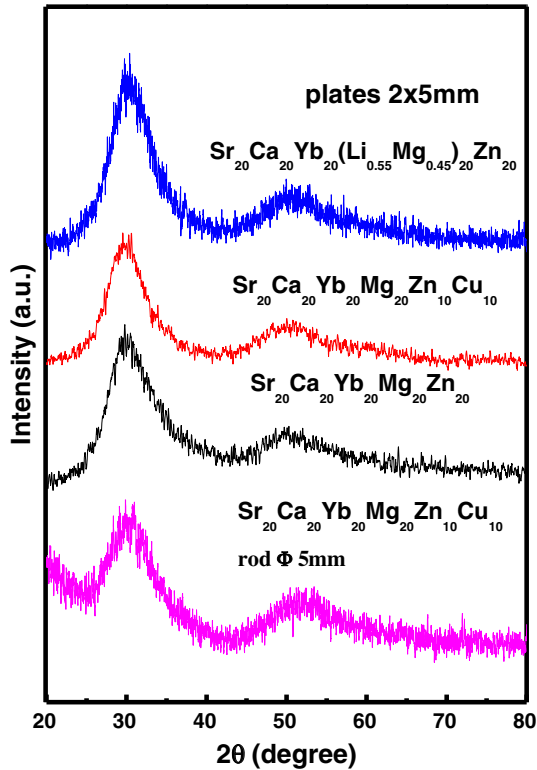


Fig. 1. XRD patterns of cross section of as-cast samples with different dimensions for  $\text{Sr}_{20}\text{Ca}_{20}\text{Yb}_{20}(\text{Li}_{0.55}\text{Mg}_{0.45})_{20}\text{Zn}_{20}$ ,  $\text{Sr}_{20}\text{Ca}_{20}\text{Yb}_{20}\text{Mg}_{20}\text{Zn}_{10}\text{Cu}_{10}$ , and  $\text{Sr}_{20}\text{Ca}_{20}\text{Yb}_{20}\text{Mg}_{20}\text{Zn}_{20}$  alloys in plate form, and  $\text{Sr}_{20}\text{Ca}_{20}\text{Yb}_{20}\text{Mg}_{20}\text{Zn}_{10}\text{Cu}_{10}$  alloy in the rod with diameter up to 5 mm.<sup>46</sup>

following multistep crystallization process consisting of three visible exothermic peaks.<sup>46</sup> The distinct glass transition and sharp crystallization events further confirm the fully amorphous structure of the high-entropy MGs. We can see that the  $T_g$ ,  $T_x$ , and the supercooled liquid region ( $\Delta T_x$ ) defined as  $\Delta T_x = T_x - T_g$  of the three high-entropy MGs are quite sensitive to the component. For  $\text{Sr}_{20}\text{Ca}_{20}\text{Yb}_{20}(\text{Li}_{0.55}\text{Mg}_{0.45})_{20}\text{Zn}_{20}$  and  $\text{Sr}_{20}\text{Ca}_{20}\text{Yb}_{20}\text{Mg}_{20}\text{Zn}_{10}\text{Cu}_{10}$ , which are obtained by substituting Li for 11% Mg and Cu for 10% Zn, respectively, the crystallization processes are simpler compared with that of  $\text{Sr}_{20}\text{Ca}_{20}\text{Yb}_{20}\text{Mg}_{20}\text{Zn}_{20}$ , which indicates that the  $\text{Sr}_{20}\text{Ca}_{20}\text{Yb}_{20}(\text{Li}_{0.55}\text{Mg}_{0.45})_{20}\text{Zn}_{20}$  and  $\text{Sr}_{20}\text{Ca}_{20}\text{Yb}_{20}\text{Mg}_{20}\text{Zn}_{10}\text{Cu}_{10}$  have simple crystal structure after crystallization because of the effect of high mixing entropy.<sup>46</sup> The  $\text{Sr}_{20}\text{Ca}_{20}\text{Yb}_{20}(\text{Li}_{0.55}\text{Mg}_{0.45})_{20}\text{Zn}_{20}$  also has much lower  $T_g$  and  $T_x$ , which can be attributed to the substitution of Li with quite low elastic moduli and melting point.<sup>45</sup> The  $\Delta T_x$  value of  $\text{Sr}_{20}\text{Ca}_{20}\text{Yb}_{20}(\text{Li}_{0.55}\text{Mg}_{0.45})_{20}\text{Zn}_{20}$  is only 25 K and much smaller than that of  $\text{Sr}_{20}\text{Ca}_{20}\text{Yb}_{20}\text{Mg}_{20}\text{Zn}_{10}\text{Cu}_{10}$  and  $\text{Sr}_{20}\text{Ca}_{20}\text{Yb}_{20}\text{Mg}_{20}\text{Zn}_{20}$ , indicating a relatively less stable glass,<sup>45</sup> which is consistent with the phenomenon of the crystallization of the glass in 7 days.

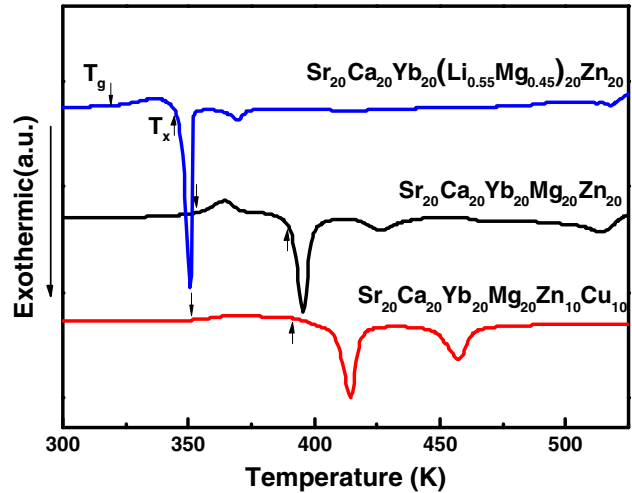


Fig. 2. The DSC curves (heating rate is 10 K/min) of as-cast  $\text{Sr}_{20}\text{Ca}_{20}\text{Yb}_{20}(\text{Li}_{0.55}\text{Mg}_{0.45})_{20}\text{Zn}_{20}$ ,  $\text{Sr}_{20}\text{Ca}_{20}\text{Yb}_{20}\text{Mg}_{20}\text{Zn}_{10}\text{Cu}_{10}$ , and  $\text{Sr}_{20}\text{Ca}_{20}\text{Yb}_{20}\text{Mg}_{20}\text{Zn}_{20}$  high-entropy MGs.

About the formation and preparation of the high-entropy MGs, we have following remarks: First, the high-entropy MGs so far can only be obtained among easy glass-forming elements. From Table I, we can see that all the high-entropy MGs involve in the conventional bulk MG-forming elements of Zr, Sr, Ca, Ti, Cu, Al, Er, Yb, Tb, Dy, Si, and B. This indicates that the formation of the high-entropy MGs should follow the empirical rules for the MG formation. Second, it is intriguing and significant if the high-entropy MGs could be obtained in some alloy system (e.g., Al, Sn, W, Mo, V, Cr, Ag, Nb, and Mn) with very poor GFA. The results would be useful for explaining the role of mixing entropy in the glass formation. Third, the amorphous high-entropy alloys can also be successfully fabricated using the solid-state reaction method of mechanical alloying.<sup>49</sup> This method could be very effective for developing more novel high-entropy MG system because the method had been demonstrated to be powerful for exploring new glassy systems. Fourth, as early as in 2002 (before the coming of the concept of the high entropy), the MG community had ever tried to develop MGs by using the idea of equal concentration of constituent elements without distinct base component. The GFA of a  $\text{Ti}_{20}\text{Zr}_{20}\text{Hf}_{20}\text{Cu}_{20}\text{Ni}_{20}$  alloy was examined both by melt-spinning and copper-mold-casting methods.<sup>52</sup> It was found that the  $\text{Ti}_{20}\text{Zr}_{20}\text{Hf}_{20}\text{Cu}_{20}\text{Ni}_{20}$  bulk glassy rod without distinct base component of 1.5 mm in diameter could be formed by copper mold casting, and the glassy alloy rod also exhibits good mechanical properties that are similar to those of ordinary glassy alloys.<sup>52</sup> It is pity, the authors did not propose the concept of high entropy, and the synthesis method of bulk glassy alloys did not draw much attention. The concept of high entropy was introduced in the MG field for exploring new MG systems until 2011.<sup>42,43,45</sup>

## The Formation Mechanism and Criteria

To understand the role of high entropy on the glass formation of an alloy, one should consider the features of the configurational entropy ( $\Delta S_{\text{conf}}$ ) or entropy of mixing in terms of atomic configurations in an alloy. According to Boltzmann's hypothesis on the relationship between the entropy and system complexity, the change in configurational entropy during the formation of a solid solution from  $n$  elements and the fraction of  $c_i$  for  $i$ th element can be described as:<sup>53</sup>

$$\Delta S_{\text{conf}} = -R \sum_{i=1}^n c_i \ln c_i \quad (1)$$

where  $R$  is the gas constant and  $\sum_{i=1}^n c_i = 1$ . For the alloys with an equimolar ratio, Eq. 1 can be expressed in following equation:<sup>53</sup>

$$\Delta S_{\text{conf}} = -R \ln \frac{1}{n} = R \ln n \quad (2)$$

From Eq. 1, the  $\Delta S_{\text{conf}}$  can be estimated as a function of alloy composition and the number  $n$  of the constituent elements, and one can see that the equiatomic composition in an alloy is of the largest value of  $\Delta S_{\text{conf}}$  at a random solid solution or amorphous state, and  $\Delta S_{\text{conf}}$  at the equiatomic composition increases with an increasing number of the components. Thus, alloys with equiatomicity or near equiatomicity and  $n \geq 5$  have a high  $\Delta S_{\text{conf}}$  state, leading to the so-called high-entropy alloy. So, the high entropy of an alloy is simply determined by as few as two factors of  $n$  and equiatomicity. The high mixing entropy promotes the tendency of simple crystal structure such as body-centered cubic (bcc) and face-centered cubic (fcc), and even amorphous structure in an alloy due to slow atomic diffusion, which can be explained by kinetic theory.<sup>46</sup> The high mixing entropy means a lower chance that the alloy can form well-defined crystal structures or the higher GFA, which is equivalent to the confusion principle<sup>12</sup> for the bulk MG formation: The amorphous phase formation is easier in multicomponent alloys with more than three alloying elements, where the mixing entropy is higher than in simpler alloy systems.

The empirical rules for the glass formation include that the alloy compositions should have three or more than three elements, and the main elements need to have larger atomic size difference (> 12%) and very negative mixing enthalpies.<sup>7,8</sup> The formation of the high-entropy MGs also follows the empirical MG formation rules. From the melting process of these alloys, we deduce that the multicomponent high-entropy MG-forming alloys are off-eutectic compositions. The reduced glass transition temperatures  $T_{\text{rg}}$  ( $T_{\text{rg}} = T_g/T_1$ ) for these alloys is quite large compared with the existing conventional bulk MG systems, which indicates the strong GFA for these high-mixing-entropy glass-forming alloys.<sup>45-51</sup>

The high mixing entropy is not a sufficient condition for the glass formation because the high entropy does not always lead to the formation of the amorphous phase or random simple solid solutions, and intermetallic compounds also form in high-entropy alloys. This indicates that apart from the entropy effect, there are other factors controlling the phase selection in the high-entropy alloy. It is suggested that the atomic size difference apparently plays a critical role in distinguishing the formation of solid solutions and the amorphous phase, and a critical parameter of the topology atomic size polydispersity  $\delta$  is defined.<sup>51</sup> The solid solutions and the amorphous phase form below and above a critical value of  $\delta$ , respectively.<sup>51</sup> The chemistry mixing enthalpy  $\Delta H_{\text{mix}}$  is regarded as another important decisive factor and a more negative  $\Delta H_{\text{mix}}$  ( $\leq 12$  kJ/mol) favors the amorphous phase formation.<sup>51</sup>

Therefore, the high-entropy concept combining the MG formation empirical rules might be a novel route in the search for new MG-forming alloy systems. It might be worth carrying out intensive efforts to investigate high-mixing-entropy MGs and to search for more amorphous alloy systems with excellent GFA and unique physical and mechanical properties.

## PROPERTIES

### Mechanical Properties

There is a mixture rule of the elastic constants of MGs that is even effective for other non-metallic glasses:<sup>54</sup> The elastic modulus of a MG ( $M$ ) can be estimated using the equation  $M = \sum f_i M_i$ , where  $M_i$  and  $f_i$  denote the elastic constant and atomic percentage of each constituent element, respectively.<sup>54</sup> The rule of mixture could also fit for other properties ( $P$ ) for a high-entropy MG with the equiatomic composition of components. That is,

$$P = \sum f_i P_i \quad (3)$$

where  $P_i$  is the certain property of the  $i$ th constituent element. That means the high-entropy MGs, depending on their composition, components, and the rule of property mixture, could exhibit unique and balance mechanical properties. Equation 3 could be used to design the desirable properties of high-entropy MGs, which is one advantage for high-entropy MGs comparing the conventional MG systems.

For example, the unique putty-like property of  $\text{Sr}_{20}\text{Ca}_{20}\text{Yb}_{20}(\text{Li}_{0.55}\text{Mg}_{0.45})_{20}\text{Zn}_{20}$  was designed and successfully fabricated using this properties mixture rule.<sup>45</sup> Table II lists the thermodynamic parameters of as-cast high-entropy MGs of  $\text{Sr}_{20}\text{Ca}_{20}\text{Yb}_{20}(\text{Li}_{0.55}\text{Mg}_{0.45})_{20}\text{Zn}_{20}$ ,  $\text{Sr}_{20}\text{Ca}_{20}\text{Yb}_{20}\text{Mg}_{20}\text{Zn}_{10}\text{Cu}_{10}$ , and  $\text{Sr}_{20}\text{Ca}_{20}\text{Yb}_{20}\text{Mg}_{20}\text{Zn}_{20}$ . These MGs have relatively low  $T_g$  close to room temperature (RT) and exhibit unique putty-like mechanical properties.

**Table II. The high-mixing-entropy SrCaYbMg-included MGs and their thermodynamic parameters, elastic moduli, and the values of glass transition temperature  $T_g$ , crystallization temperature  $T_x$ , and liquidus temperature  $T_l$ <sup>45,46</sup>**

Alloy system	Sr <sub>20</sub> Ca <sub>20</sub> Yb <sub>20</sub> Mg <sub>20</sub> Zn <sub>20</sub>	Sr <sub>20</sub> Ca <sub>20</sub> Yb <sub>20</sub> Mg <sub>20</sub> Zn <sub>10</sub> Cu <sub>10</sub>	Zn <sub>20</sub> Sr <sub>20</sub> Ca <sub>20</sub> Yb <sub>20</sub> (Li <sub>0.55</sub> Mg <sub>0.45</sub> ) <sub>20</sub>
$T_g$ (K)	353	351	319
$T_x$ (K)	389	391	344
$T_l$ (K)	630	642	559
$\Delta T_x$ (K)	36	40	25
$T_{rg}$	0.56	0.55	0.57
$E$ (GPa)	22.8	24.3	16.1
$G$ (GPa)	8.89	9.47	6.28
$K$ (GPa)	17.5	18.6	12.4
$\nu$	0.283	0.282	0.283

It is known that the plastic deformation behavior in a MG is related to the strain rate and the ratio of test temperature ( $T_t$ ) to  $T_g$ ,  $T_r$  ( $= T_t/T_g$ ).<sup>45</sup> Theoretically, the homogeneous flow of MGs could take place below  $T_g$  at extreme low strain rates or high  $T_r$  ( $> 0.85$ ).<sup>55</sup> The low  $T_g$  of a MG, which corresponds to a high value of  $T_r$  ( $T_r = T_t/T_g = RT/T_g$ ) could enhance the plasticity of the MGs at RT. To increase the  $T_r$  for the alloy, one can decrease its  $T_g$  based on the correlation between the  $T_g$  and elastic moduli of MGs.<sup>55</sup> The lower elastic moduli gives lower  $T_g$ . According to the mixture rule of property of Eq. 3: The elastic constants of MGs show a correlation with a weighted average of the elastic constants for the constituent elements. One can add Li, Ca, Sr, and Mg elements, which have low elastic modulus, while all the Ca, Sr, Li, and Mg are active elements. The Zn was also chosen for addition, which has been proven to be effective for improving the corrosion resistance of MGs.<sup>10</sup> Combining with the confusion principle, high mixing entropy rule, and property mixture rule, the alloy with six components with similar fraction was designed to achieve enhanced GFA and very low  $T_g$ , which leads to putty-like homogeneous plasticity at RT.<sup>45</sup>

Figure 3a shows the compressive stress–strain curves of as-cast high-entropy MG rods (2 mm in diameter) of Sr<sub>20</sub>Ca<sub>20</sub>Yb<sub>20</sub>(Li<sub>0.55</sub>Mg<sub>0.45</sub>)<sub>20</sub>Zn<sub>20</sub>, Sr<sub>20</sub>Ca<sub>20</sub>Yb<sub>20</sub>Mg<sub>20</sub>Zn<sub>10</sub>Cu<sub>10</sub>, and Sr<sub>20</sub>Ca<sub>20</sub>Yb<sub>20</sub>Mg<sub>20</sub>Zn<sub>20</sub> at RT.<sup>45</sup> For the Sr<sub>20</sub>Ca<sub>20</sub>Yb<sub>20</sub>Mg<sub>20</sub>Zn<sub>10</sub>Cu<sub>10</sub> and Sr<sub>20</sub>Ca<sub>20</sub>Yb<sub>20</sub>Mg<sub>20</sub>Zn<sub>20</sub> MGs, their values of fracture strength are 423 MPa and 382 MPa, respectively. After elastic deformation, almost no plastic deformation occurred in the two bulk metallic glasses (BMGs). While for Sr<sub>20</sub>Ca<sub>20</sub>Yb<sub>20</sub>(Li<sub>0.55</sub>Mg<sub>0.45</sub>)<sub>20</sub>Zn<sub>20</sub> MG with very low  $T_g$  (319 K) and high  $T_r$  ( $> 0.90$ ), after the elastic strain limit of  $\sim 2\%$  (the yield strength  $\sigma_y$  is about 383 MPa), it remarkably displays stress overshoot as is often observed in homogeneous deformation in the supercooled liquid state, which is generally thought to be caused by the change in free volume or activation of flow units during deformation.<sup>56–60</sup> After the overshoot, the stress  $\sigma$  attains a steady state as shown in Fig. 3a.

The exceptional deformability and flexibility observed in supercooled liquid state at RT is due to its ultralow value of  $T_g$  or ultrahigh  $T_r$ .<sup>42</sup> When the strain rate decreases to  $10^{-5} \text{ s}^{-1}$ , the yielding stress and steady flow stress decrease as shown in Fig. 3b. As shown in the picture of Fig. 3c, the sample can be compressed to 70% of its original height without observable cracking and shear banding, and further compression is still possible to extend the deformation.<sup>45</sup> Such a heavy deformation without shear bands and fracture, and the strain-rate dependence of the steady-state flow stress indicates the homogeneous flowability of the MG at RT. Previously, such exceptional deformability and flexibility can only be obtained in supercooled liquid state at high temperatures and has never been observed at RT for conventional MGs, which would fail after little observable plastic strain.<sup>45</sup> The x-ray diffraction examination verifies that the severe deformed samples remain fully amorphous.<sup>42</sup> The MGs are often called as “liquid metals,” and the finding of the viscoplastic high-entropy MG makes the term of “liquid metals” a reality because of the significant viscoplastic flow at RT. The apparent viscosity of the MG at RT is estimated to be about  $10^{12} \text{ Pa s}$ , which is close to the viscosity of supercooled liquid state near  $T_g$ .<sup>45</sup> The high-entropy MG indeed stands at the boundary between the solid and liquid, and it offers a model system to study some fundamental issues, such as glass transition and plastic flow mechanism. For example, because of the stable metallic supercooled liquids near RT, it is possible to observe the intrinsic viscous behavior of the MG or supercooled liquid state around RT.

### Putty-Like Molding and Imprinting Properties

The molding and imprinting previously reported for oxide glasses and conventional MGs have to be performed at higher temperatures.<sup>61</sup> For oxide glasses, for example,  $T_g > 1000 \text{ K}$ , and for Zr-, Fe-, Cu-based MGs,  $T_g$  is above 500 K and even more. Because of the high  $T_g$ , molding of conventional

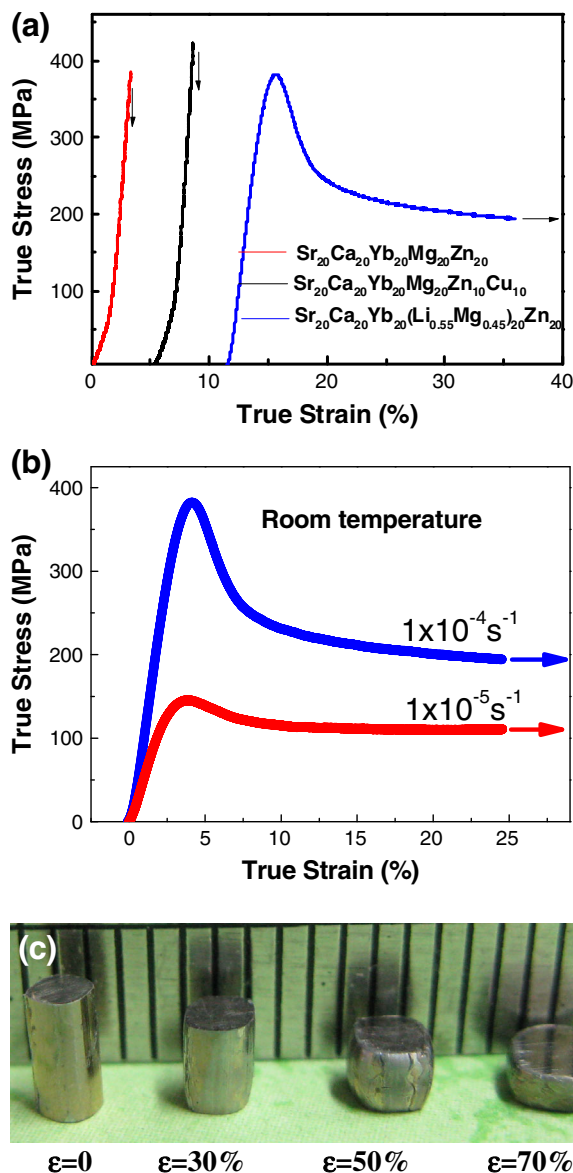


Fig. 3. (a) The compressive stress–strain curves of as-cast rods for  $\text{Sr}_{20}\text{Ca}_{20}\text{Yb}_{20}(\text{Li}_{0.55}\text{Mg}_{0.45})_{20}\text{Zn}_{20}$ ,  $\text{Sr}_{20}\text{Ca}_{20}\text{Yb}_{20}\text{Mg}_{20}\text{Zn}_{10}\text{Cu}_{10}$  and  $\text{Sr}_{20}\text{Ca}_{20}\text{Yb}_{20}\text{Mg}_{20}\text{Zn}_{20}$  high-entropy MGs. (b) The stress–strain curves for  $\text{Zn}_{20}\text{Ca}_{20}\text{Sr}_{20}\text{Yb}_{20}(\text{Li}_{0.55}\text{Mg}_{0.45})_{20}$  at strain rates of  $10^{-4} \text{ s}^{-1}$  and  $10^{-5} \text{ s}^{-1}$ . (c) The photo image of the compressed MG, which can be compressed up to 70% of its original height without shear banding and cracking.<sup>45</sup>

MGs is often performed as part of the original quench, in a squeezing-casting or high-pressure casting process.<sup>61</sup> In contrast, the  $\text{Ca}_{20}\text{Sr}_{20}\text{Yb}_{20}(\text{Li}_{0.55}\text{Mg}_{0.45})_{20}\text{Zn}_{20}$  BMG has relatively larger supercooled liquid region compared with conventional MG ribbons and ultralow  $T_g$ , which makes the high-entropy MG show polymer-like thermoplastic formability near or even at RT. Figure 4 shows the square array of MG imprinted at room temperature, which indicates the super

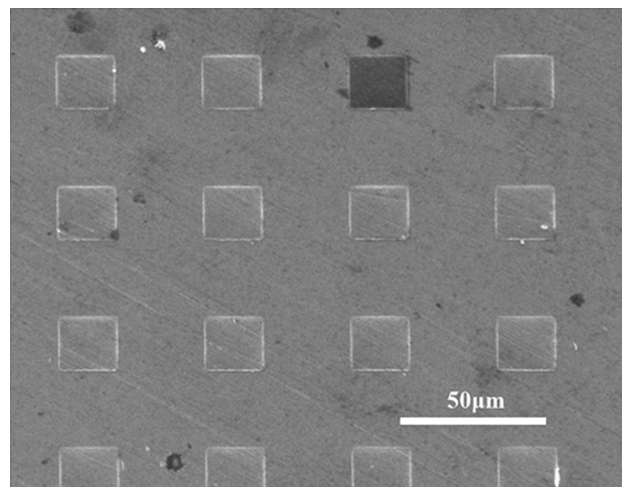


Fig. 4. Square array of the high-entropy  $\text{Sr}_{20}\text{Ca}_{20}\text{Yb}_{20}(\text{Li}_{0.55}\text{Mg}_{0.45})_{20}\text{Zn}_{20}$  MG imprinted in air condition at room temperature.

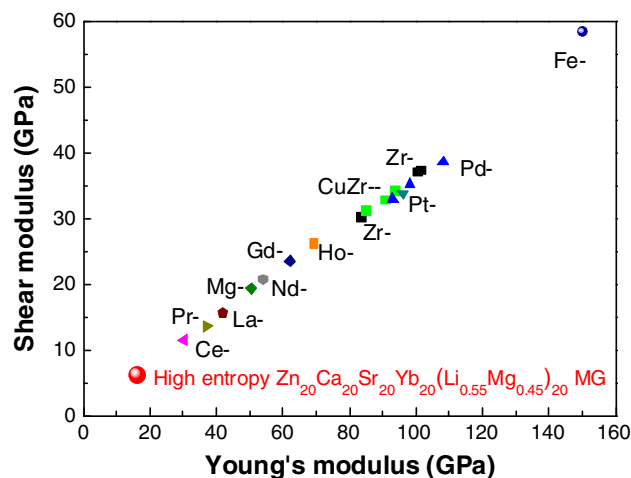


Fig. 5. The comparison of the Young's modulus and shear modulus of a series MGs. The  $\text{Zn}_{20}\text{Ca}_{20}\text{Sr}_{20}\text{Yb}_{20}(\text{Li}_{0.55}\text{Mg}_{0.45})_{20}$  BMG has the smallest elastic constant among other typical BMGs.<sup>45</sup>

thermoplastic formability of the MG.<sup>46</sup> The high-entropy MG can be repeatedly compressed, stretched, bent, and formed into complicated shapes, including nanoimprinted patterns demonstrating the excellent thermoplastic processability as the conventional polymeric materials.<sup>62</sup> It is expected that with careful design of composition using the high-entropy concept, more similar plastic-like MGs could be developed based on multiple principal elements.

### Elastic Properties

The elastic moduli were determined from acoustic velocities measurements, and the results are listed in Table II. The value of Poisson's ratio  $\nu$  for the three  $\text{Sr}_{20}\text{Ca}_{20}\text{Yb}_{20}(\text{Li}_{0.55}\text{Mg}_{0.45})_{20}\text{Zn}_{20}$ ,  $\text{Sr}_{20}\text{Ca}_{20}\text{Yb}_{20}\text{Mg}_{20}\text{Zn}_{10}\text{Cu}_{10}$ , and  $\text{Sr}_{20}\text{Ca}_{20}\text{Yb}_{20}\text{Mg}_{20}\text{Zn}_{20}$

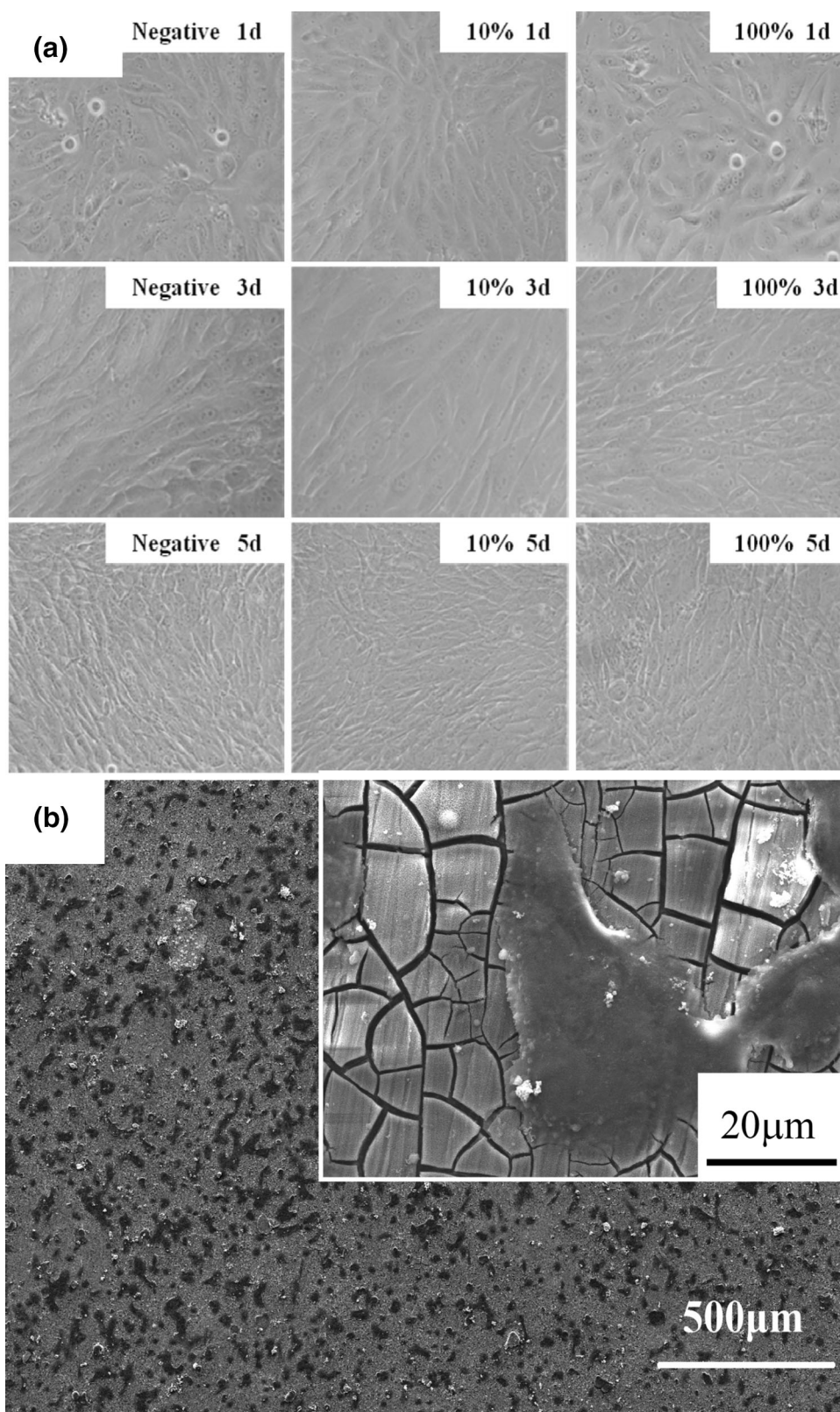


Fig. 6. (a) Optical morphologies of MG63 cells ( $15 \times 15 \mu\text{m}^2$  scan range) that were cultured in the negative control and 10%, 100% concentration  $\text{Sr}_{20}\text{Ca}_{20}\text{Yb}_{20}\text{Mg}_{20}\text{Zn}_{20}$  MG extraction mediums for 1, 3, and 5 days. (b) The morphology of MG63 cells cultured on  $\text{Sr}_{20}\text{Ca}_{20}\text{Yb}_{20}\text{Mg}_{20}\text{Zn}_{20}$  MG directly for 1 day.<sup>47</sup>



MGs is almost the same. The elastic moduli such as  $G$  and  $E$  are ultralow compared with that of other conventional bulk MGs. The elastic constants of MGs can be estimated using the mixture rule.<sup>54</sup> Therefore, the substitution of Li for Mg, which has very low elastic moduli, makes the modulus of  $\text{Sr}_{20}\text{Ca}_{20}\text{Yb}_{20}(\text{Li}_{0.55}\text{Mg}_{0.45})_{20}\text{Zn}_{20}$  remarkably low, which causes the ultralow elastic moduli. The obtained high-entropy MG indeed has low elastic moduli, and the Young's modulus  $E$ , shear modulus  $G$ , bulk modulus  $B$ , and Poisson ratio  $\nu$  measured by ultrasonic method at RT using a pulse echo overlap method (with a carry frequency of 10 MHz<sup>20</sup>) are 16 GPa, 6.3 GPa, 12 GPa, and 0.28 GPa, respectively. Figure 5 shows the comparisons of  $E$  and  $G$  between  $\text{Zn}_{20}\text{Ca}_{20}\text{Sr}_{20}\text{Yb}_{20}(\text{Li}_{0.55}\text{Mg}_{0.45})_{20}$  and other MGs. It shows clearly that the elastic constants of  $\text{Zn}_{20}\text{Ca}_{20}\text{Sr}_{20}\text{Yb}_{20}(\text{Li}_{0.55}\text{Mg}_{0.45})_{20}$  are the lowest in known MGs so far.

The RT homogeneous deformation of the glass can be understood from the ultralow elastic moduli of the high-entropy MG. According to elastic model,<sup>63</sup> the flow barrier energy  $W$  of flow units in MGs can be estimated by  $W \propto GV_m$ , where  $V_m$  is average molar volume of the flow units. The MGs with lower  $W$  generally have good ductility. Because of the ultralow  $G$  (6.3 GPa), the MGs have much lower activation energy for flow units compared with that of other known MGs. The activation of flow units is then much easier, which leads to the homogenous flow in the high-entropy MG. This is the case of applied stress-induced glass transition at RT, which confirms the similarity and correlation between the plastic flow and the glass transition in MGs.<sup>63–66</sup> On the other hand, the results indicate that the decrease of  $T_g$  or  $G$  by design is another route for the design of ductile MGs.

### Other Properties

The property of the high-entropy MGs with the equiatomic composition of components could have mixture or combining properties of the components depending on their components and following the rule of property mixture of Eq. 3. Another example is that the  $\text{FeSiAlNiNb}$  amorphous high-entropy alloy formed by the mechanical alloying method shows the higher thermal stability due to the component of Nb, B, and soft-magnetic property with low coercivity due to the components of Fe and Ni.<sup>46</sup> The  $\text{Pd}_{20}\text{Pt}_{20}\text{Cu}_{20}\text{Ni}_{20}\text{P}_{20}$  high-entropy MG has very high GFA because the Pd and Pt components can alloy with Ni and P with high GFA.<sup>48</sup> The  $\text{Ti}_{20}\text{Zr}_{20}\text{Cu}_{20}\text{Ni}_{20}\text{Be}_{20}$  high-entropy MG exhibits high fracture strength of 2315 MPa because Ti, Zr, and Ni components have high strength.<sup>50</sup>

The  $\text{CaMgZnSrYb}$  high-entropy MG is a biomedical degradable material<sup>45–47</sup> because of its low density and low Young's modulus that is comparable to the modulus of human bones (the attributes are the result of the low density and moduli of Ca,

Mg, and Sr components). It is a biomedical degradable material<sup>45–47</sup> due to the biological effect/function of component elements Ca, Mg, and Zn: Calcium is a major component in human bone and calcium is also essential in chemical signaling with cells. Magnesium is essential to human metabolism and is the fourth most abundant cation in the human body. Magnesium is a cofactor for many enzymes and stabilized the structures of DNA and RNA. Zinc is the second most prevalent trace element in the human body and is reported to stimulate fracture healing of bone, reduce postmenopausal bone loss, improve bone mineralization, and improve skeletal strength. Moreover, Zn is an effective agent in killing bacterial strains commonly associated with infection in orthopedic surgeries.

The developed  $\text{CaMgZnSrYb}$  high-entropy MG can be considered as a biomedical degradable material<sup>45,47</sup> because it shows higher compression strength ( $371 \pm 25$  MPa) than cortical bone (150–250 MPa) and has similar Young's modulus ( $16.1 \pm 0.1$  GPa) to cortical bone (5–25 GPa), and it has much better corrosion resistance due to the elements Sr and Yb. The indirect and direct cytocompatibility tests showed that Ca-included high-entropy MG samples have satisfactory cell viability and alkaline phosphatase activity, and the human osteoblast-like cells (MG63 cells) are found to be well adhered on the surface of the MG indicating their healthy status (due to the Ca component).<sup>47</sup> Figure 6a and b show the morphologies of MG63 cells cultured in the extraction media and  $\text{CaMgZnSrYb}$  bulk MGs' surfaces.<sup>47</sup> Most of the cells were flattened, had polygonal configuration and dorsal ruffles, and were well attached to the substrate by cellular extension, indicating their healthy status.

All the examples above demonstrate that the introducing of concept of high entropy into the field of MGs could lead to unique and combining properties that conventional alloys lack, which gives them good potential for many applications.

### CONCLUSION AND OUTLOOK

In conclusions, high-mixing-entropy MGs with high GFA can be prepared using various conventional MG casting methods. Compared with the conventional alloy development strategy leading to an enormous amount of knowledge about alloys based on one or two components, there is little knowledge about MGs containing several main components in near-equal proportions. We show that the high-mixing-entropy MGs, along the formation idea and strategy of the high-entropy alloys and based on multiple major elements, provide a novel and effective approach for the design and search of new MG-forming alloy systems with significances in scientific studies and potential applications.

The high mixing entropy can enhance the GFA in certain cases, but it is not a sufficient condition for glass formation. The high-entropy MGs so far can only be obtained among easy glass-forming elements, and the high-entropy effect is mainly related to the well-known confusion principle for the glass formation. It is suggested that the atomic size difference apparently plays a critical role in distinguishing the formation of crystalline solid solutions and the amorphous phase.

High-entropy alloy design could make use of the mixture of the various properties of the various components, and leads to the unique and combining physical and mechanical properties. These obtained high-entropy MGs (the system is limited) indeed have unique physical and mechanical properties, and they could offer an ideal model to investigate some fundamental issues such the glass transition and deformation mechanism in MGs.

It is expected that with careful design of composition using the high-entropy concept, easy glass formation should be possible in a variety of alloys based on multiple principal elements. It seems likely that the high-entropy MGs still have more surprises in the future.

#### ACKNOWLEDGEMENTS

The experimental aid and discussions of K. Zhao, X.Q. Gao, H.Y. Bai, D.Q. Zhao, D.W. Ding, M.X. Pan, H.F. Li, and Y. F. Zheng are greatly appreciated. Financial support from NSF of China (51271195) and MOST973 of China (2007CB613904 and 2010CB731603) are acknowledged.

#### REFERENCES

- W. Clement, R.H. Willens, and P. Duwez, *Nature* 187, 869 (1960).
- H.S. Chen, *Rep. Prog. Phys.* 43, 353 (1980).
- W.H. Wang, C. Dong, and C.H. Shock, *Mater. Sci. Eng. R* 44, 45 (2004).
- W.L. Johnson, *Prog. Mater. Sci.* 30, 81 (2007).
- W.H. Wang, *Adv. Mater.* 21, 4524 (2009).
- H.A. Daveis, *Amorphous Metallic Alloys*, ed. F.E. Luborsky (London, UK: Butterworths, 1983), p. 8.
- A. Peker and W.L. Johnson, *Appl. Phys. Lett.* 63, 2342 (1993).
- A. Inoue, *Mater. Trans. JIM* 36, 866 (1995).
- Y. Li, S.J. Poon, J. Xu, D.H. Kim, and J.F. Loeffler, *MRS Bull.* 32, 624 (2007).
- W.H. Wang, *Prog. Mater. Sci.* 52, 540 (2007).
- P. Yu, H.Y. Bai, and W.H. Wang, *J. Mater. Res.* 21, 1674 (2006).
- A.L. Greer, *Nature* 366, 303 (1993).
- Q. Luo and W.H. Wang, *J. Non-Cryst. Solids* 355, 759 (2009).
- A. Inoue, N. Nishiyama, and H. Kimura, *Mater. Trans. JIM* 38, 179 (1997).
- S. Li, R.J. Wang, and W.H. Wang, *J. Non-Cryst. Solids* 354, 1080 (2008).
- F.Q. Guo, S.J. Poon, and G.J. Shiflet, *Scr. Mater.* 43, 1089 (2000).
- M.B. Tang, D.Q. Zhao, and W.H. Wang, *Chin. Phys. Lett.* 21, 901 (2004).
- W.H. Wang, J.J. Lewandowski, and A.L. Greer, *J. Mater. Res.* 20, 2307 (2005).
- B. Zberg, P.J. Uggowitzer, and J.F. Löffler, *Nature Mater.* 8, 887 (2009).
- B. Zhang, D.Q. Zhao, M.X. Pan, W.H. Wang, and A.L. Greer, *Phys. Rev. Lett.* 94, 205502 (2005).
- K. Zhao, J.F. Li, D.Q. Zhao, and W.H. Wang, *Scr. Mater.* 61, 1091 (2009).
- Z.P. Lu, C.T. Liu, J.R. Thompson, and W.D. Porter, *Phys. Rev. Lett.* 92, 245503 (2004).
- Y.H. Liu, G. Wang, R.J. Wang, M.X. Pan, and W.H. Wang, *Science* 315, 1385 (2007).
- W.H. Wang, M.X. Pan, and H.Y. Bai, *J. Phys. Condens. Mat.* 16, 3719 (2004).
- D. Meng, J. Yi, D.Q. Zhao, D.W. Ding, H.Y. Bai, and W.H. Wang, *J. Non-Cryst. Solids* 357, 1787 (2011).
- E.S. Park and D.H. Kim, *J. Mater. Res.* 19, 685 (2004).
- Z.F. Zhao, D.Q. Zhao, and W.H. Wang, *Appl. Phys. Lett.* 82, 4699 (2003).
- J. Schroers and W.L. Johnson, *Appl. Phys. Lett.* 84, 3666 (2004).
- J. Das, M.B. Tang, K.B. Kim, W.H. Wang, and J. Eckert, *Phys. Rev. Lett.* 94, 205501 (2005).
- V. Ponnambalam, S.J. Poon, and G.J. Shiflet, *J. Mater. Res.* 19, 1320 (2004).
- K.B. Kim, P.J. Warren, and B. Cantor, *J. Non-Cryst. Solids* 317, 17 (2003).
- J.F. Li, D.Q. Zhao, M.L. Zhang, and W.H. Wang, *Appl. Phys. Lett.* 93, 171907 (2008).
- X.F. Liu, R.J. Wang, D.Q. Zhao, M.X. Pan, and W.H. Wang, *Appl. Phys. Lett.* 91, 041901 (2007).
- J.W. Yeh, S.K. Chen, and S.J. Lin, *Adv. Eng. Mater.* 6, 299 (2004).
- B. Cantor, I.T.H. Chang, and P. Knight, *Mater. Sci. Eng. A* 375–377, 213 (2004).
- Y. Zhang, T.T. Zuo, Z. Tang, M.C. Gao, K.A. Dahmen, P.K. Liaw, and Z.P. Lu, *Prog. Mater. Sci.* 61, 1 (2014).
- J.W. Yeh, *Ann. Chim. Sci. Mater.* 31, 633 (2006).
- O.N. Senkov, G.B. Wilks, J.M. Scott, and D.B. Miracle, *Intermetallics* 19, 698 (2011).
- Y. Zhang, X. Yang, and P.K. Liaw, *JOM* 64, 830 (2012).
- Y.J. Zhou, Y. Zhang, Y.L. Wang, and G.L. Chen, *Appl. Phys. Lett.* 90, 181904 (2007).
- F. Tian, L. Delczeg, N. Chen, L.K. Varga, J. Shen, and L. Vitos, *Phys. Rev. B* 88, 085128 (2013).
- M.C. Gao and D.E. Alman, *Entropy* 15, 4504 (2013).
- M. Widom, W.P. Huhn, S. Maiti, and W. Steurer, *Metall. Mater. Trans. A* 45, 196 (2014).
- N.-P. Ong and R. Bhatt, *More is Different* (Princeton, NJ: Princeton University Press, 2001).
- K. Zhao, H.Y. Bai, D.Q. Zhao, and W.H. Wang, *Appl. Phys. Lett.* 98, 141913 (2011).
- X.Q. Gao, K. Zhao, H.B. Ke, D.W. Ding, W.H. Wang, and H.Y. Bai, *J. Non-Cryst. Solids* 357, 3557 (2011).
- H.F. Li, X.H. Xie, K. Zhao, Y.B. Wang, Y.F. Zheng, W.H. Wang, and L. Qin, *Acta Biomater.* 9, 8561 (2013).
- A. Takeuchi, N. Chen, T. Wada, Y. Yokoyama, H. Kato, and A. Inoue, *Intermetallics* 19, 1546 (2011).
- J. Wang, Z. Zheng, J. Xu, and Y. Wang, *J. Magn. Magn. Mater.* 355, 58 (2014).
- H.Y. Ding and K.F. Yao, *J. Non-Cryst. Solids* 364, 9 (2013).
- S. Guo, Q. Hu, C. Ng, and C.T. Liu, *Intermetallics* 41, 96 (2013).
- L.Q. Ma, L.M. Wang, T. Zhang, and A. Inoue, *Mater. Trans.* 43, 277 (2002).
- R.A. Swalin, *Thermodynamics of Solids* (New York: Wiley, 1991).
- W.H. Wang, *J. Appl. Phys.* 99, 093506 (2006).
- P.S. Steif, F. Spaepen, and J.W. Hutchinson, *Acta Metall.* 30, 447 (1982).
- J.S. Langer, *Phys. Rev. E* 70, 041502 (2004).
- S.T. Liu, W. Jiao, B.A. Sun, and W.H. Wang, *J. Non-Cryst. Solids* 376, 76 (2013).

58. Z. Wang, P. Wen, L.S. Huo, H.Y. Bai, and W.H. Wang, *Appl. Phys. Lett.* 101, 120906 (2012).
59. S.T. Liu, Z. Wang, H.L. Peng, H.B. Yu, and W.H. Wang, *Scr. Mater.* 67, 9 (2012).
60. W. Jiao, P. Wen, H.L. Peng, H.Y. Bai, B.A. Sun, and W.H. Wang, *Appl. Phys. Lett.* 102, 101903 (2013).
61. G. Kumar, H.X. Tang, and J. Schroers, *Nature* 460, 457 (2009).
62. N. March and M. Tosi, *Polymers, Liquid Crystals and Low-Dimensional Solids* (New York: Plenum, 1984), p. 3.
63. W.H. Wang, *Prog. Mater. Sci.* 57, 487 (2012).
64. Y.H. Liu, C.T. Liu, W.H. Wang, A. Inoue, and M.W. Chen, *Phys. Rev. Lett.* 103, 065504 (2009).
65. B. Yang, J. Wadsworth, and T.G. Nieh, *Appl. Phys. Lett.* 90, 061911 (2007).
66. W.H. Wang, *J. Appl. Phys.* 110, 053521 (2011).